應用於高頻與低雜訊具有砷化銦鎵/砷化銦 超晶格通道之變質型高電子遷移率電晶體之研究

研究生：曾文仲　　　　　　　　　　　　　　　　指導教授：張 翼 博士

國立交通大學材料科學與工程研究所

摘要

本次研究中探討使用砷化銦鎵/砷化銦 超晶格為通道層之 InAlAs/InGaAs 變質型高電子遷移率電晶體(MHEMTs)在高頻的應用。

利用砷化銦鎵/砷化銦超晶格通道在變質型砷化鎵基板上能夠有效提升通道層的銦含量。此外在超晶格結構中，由於電子減少與通道中銦原子或鎵原子的不規則散射，因而擁有比傳統砷化銦鎵通道較好的電子傳輸性質。此外砷化銦的能階較低，通道中的較多電子會被限制在砷化銦量子井中，使得整個元件的電子傳輸特性將以砷化銦為主，因此能夠有效提升使用超晶格通道之變質型高電子遷移率電晶體的電子特性

在元件特性方面，使用超晶格通道之變異型 100 nm 高電子遷移率電晶體其在此次的研究中其汲極飽和電流密度為 476 mA/mm，而電流在 0.9 V 的汲極偏壓下最大的互導係數可達 886 mS/mm。元件的電流增益截止頻率及最大共振頻率皆為 170 GHz。雜訊方面，元件在 16GHz 的頻率下，雜訊值為 0.77 dB。

因此，本次研究成功的研發出在變質型砷化鎵基板上，利用超晶格結構，能有效提高通道層中的銦含量，並且應用此結構之元件具有優越的電流以及高頻低雜訊的特性。

Study of InGaAs/InAs Superlattice Channel Metamorphic HEMT (MHEMT) for High-frequency and Low-noise Applications

Student: Wen-Chung Tsern Advisor: Dr. Edward Yi Chang

Department of Materials Science and Engineering

National Chiao Tung University

Abstract

In this dissertation, the feasibility of using ($In_{0.53}Ga_{0.47}As$)/(InAs) superlattice as the channel in the InAlAs/InGaAs metamorphic high electron mobility transistors (MHEMT) for high frequency applications is studied.

The indium content in the channel can effectively be increased by using the InGaAs/InAs superlattice structure on metamorphic GaAs substrate. In addition, because of the reduction of electron disorder scattering by composite In and Ga atoms in the channel, the electron transport properties in the superlattice structure are enhanced. Furthermore, more electrons are confined in the InAs quantum wells in the superlattice channel due to the low bandgap of InAs. Consequently, the performance of MHEMT with superlattice channel is improved.

In this study, the metamorphic HEMT with superlattice channel exhibit excellent performance such as I_{DSS} of 476 mA/mm, g_m of 886 mS/mm at drain bias voltage of 0.9V with gate length of 100 nm. The device also demonstrates a cutoff frequency f_T of 170 GHz and a maximum frequency of oscillation f_{max} up to 170 GHz. The noise figure of the device is 0.77 dB at 16GHz.

Consequently, a high indium content superlattice channel HEMT on metamorphic GaAs substrate is successful developed, and the device exhibits superior DC and RF performance than conventional InGaAs metamorphic HEMT for high frequency application.

誌謝

隨著論文一點一滴的逐步完成，心中的感觸也越來越多。從兩年前剛離開大學生活的那種懵懵懂懂，到如今即將要結束充實的碩士班生活，邁向人生下一個階段。說到要感謝誰，那真的是無法用三言兩語來說明。

首先，當然是先感謝實驗室中的大家長，張翼教授。在碩士班兩年的生活中，老師提供我們完善的儀器設備，讓我們在研究方面能夠有相當充裕的資源可以運用，此外悉心的指導以及過人的見解，令我在過去兩年的生活中受益良多。在這最後的幾個月，也多謝了老師在各方面的照顧，讓我深深感受到老師除了是嚴師也是慈父。

接著，要感謝是指導我的建億學長、家源學長以及仕鴻學長。想到第一次見到建億學長的時候，還常常因為他嚴肅的表情而有所害怕。但是日子久了，了解到他是個相當認真負責而且對人又親切的學長。在碩士班最後幾個月的生活，也多虧了建億學長如此辛勞的幫助，讓我的研究能夠順利的完成，心中滿滿的感謝已經無法用文字來描寫，想到過去那段時間，眼眶也不經意地泛起淚光；家源學長除了在實驗上無時無刻的細心指導外，在日常生活中也是可以聊心裡話的好朋友；仕鴻學長為人親切，雖然不善言語但對人總是相當親切；此外學長學富五車，當思路遇到困難時，都能適當的給予我幫助。

瑞乾學長及炎璋學長，一直以來都是我打球的好夥伴好朋友，無論是實驗以及待人處事方面，都能夠給我最真誠的建議。岳欽學長、宗育學長、家達學長、芳茗學長、雲冀學長、克弦學長，感謝你們在各個方面的幫助，若沒有你們，整個研究也不會那麼順利完成。

此外感謝同屆的士軒、渼璇及吟竹同學，在最後這幾個月，大家一起努力一起加油，一起度過總總難關，希望各位都能夠有美好的前途。雖然士軒同學已經直升為博士班，但是還是與我們一起努力，也給予我們許多的歡樂，讓我們緊張的心情能夠獲得暫時的解放。

感謝偉進、佑霖學弟，一起玩樂，一起悲傷，雖然只有短短一年的時間，但是這段日子真的是讓人特別難忘。雖然我們是學長學弟們的關係，但總是像好兄弟一般。即將要離開了，心中擁有著無限的感觸，我永遠會記得一起喝酒，一起吃鴨肉許，一起玩勁爆骰子樂。在此也祝兩位在往後直升博士班的日子順順利利。

感謝一路上給予我支持的朋友。謝謝你們，即使是少少的一句話，也讓我感到你們的關心及鼓勵。

最後感謝陪伴我這一路走來的家人們。首先，感謝我的女友令涵，感謝妳能夠無怨無悔的包容我的暴躁、無趣，忍受我因為實驗而常常不能陪伴妳，忍受我。兩年的時光不算短，這段時間真的是非常辛苦妳了。此外感謝我的媽媽。感謝你們在我完成學業的這段時間能夠讓我沒有後顧之憂，給予我強大的後盾，讓我能夠順利完成，也請原諒我無法時常在妳身邊照顧妳。媽媽，謝謝您。

最後，感謝那些我沒有感謝到的人。謝謝各位，請原諒我僅用三言兩語草草帶過心中的感激，並附上最大的祝福，願各位萬事順心，實驗室的學長及學弟們都能夠順利畢業。

Contents

Abstract (Chinese)…………………………………………………………...............I

Abstract (English)……………………………………………………………..III

Acknowledge………………………………………………………………….....IV

Contents……………………………………………………………..............VI

Tables Captions…………………………………………………………........VIII

Figures Captions……………………………………………………..……..IX

Chapter 1 Introduction

1.1 General Background…………………………………………………… .1

1.2 Overview of High Electron Mobility Transistors (HEMTs)……………..…...1

1.3 The methods to improve device performance for high frequency

Application……………………………………………………………….…..4

1.4 Motivation and dissertation outline………………………………………….. 5

..

Chapter 2 Study of Superlattice Channel

2.1 Indium-rich InGaAs channel vs. critical thickness ………………...…….. .9

2.2 High Indium content superlattice channel…………………………………10

Chapter3 Fabrication and DC & RF measurement of MHEMT

3.1 Device structure…………………………………………………………13

3.2 Device Fabrication ……………………………………………………...…13

3.2.1 Mesa/Device isolation…………………………………………….…..…14

3.2.2 Ohmic contact Formation……………………………………………..…15

3.2.3 T-shaped gate process……………………………………………..…..15

3.2.4 Device passivation and contact via formation……………………….…17

3.2.5 Airbridge formation…………………………………………..……17

3.3 Device Characterization ………………………………………...……20

3.3.1 I-V characteristics…………………………………………………..…21

3.3.2 Transmission line model (TLM)……………………………………….…24
3.3.3 Breakdown characteristics……………………………………………...25
3.4 RF Characteristics & Measurements……………………………….…26
3.4.1 Scattering parameters …………………………………………….…26
3.4.2 Current gain cutoff frequency f_T……………………………….…28
3.4.3 Maximum frequency of oscillation f_{max} ……………………………...29
3.5. Noise figure ……………………………………………………...32

Chapter 4 Results and discussions
4.1 DC characteristics………………………………………………....49
4.1.1 *I*-*V* characteristics…………………………………………..……49
4.1.2 Breakdown voltage……..………………………………………….50
4.1.3 Impact ionization effect
4.2 RF characteristics………….……………………………………….50
4.2.1 Unit current gain cut-off frequency (f_T) & maximum frequency of oscillation (f_{max}) ………….………………………………………...51
4.2.2 Noise characteristics ……..…………………………………………..52
4.3 Summary ……………..…………………………………………….52

Chapter 5 Conclusion……………………………………………………62

Chapter 6 References……..……………………………………………64

Tables

Table 1-1 Comparison of lattice-matched InP HEMT and metamorphic GaAs HEMT. ………………………………………………… ………… 6

Table 1-2 Channel material properties at 295K …………………………… 7

Table 1-3 Best performance of InP HEMT and GaAs-based metamorphic HEMT published in recent years. ……………………………………… 7

Table 4-1 Summary of the DC performances between Sample A and Sample B ……………………………………………………. 54

Table 4-2 Summary of RF performances between samples A and B ……... 54

Table 4-3 Summary of noise figure between samples A and B ……………. 54

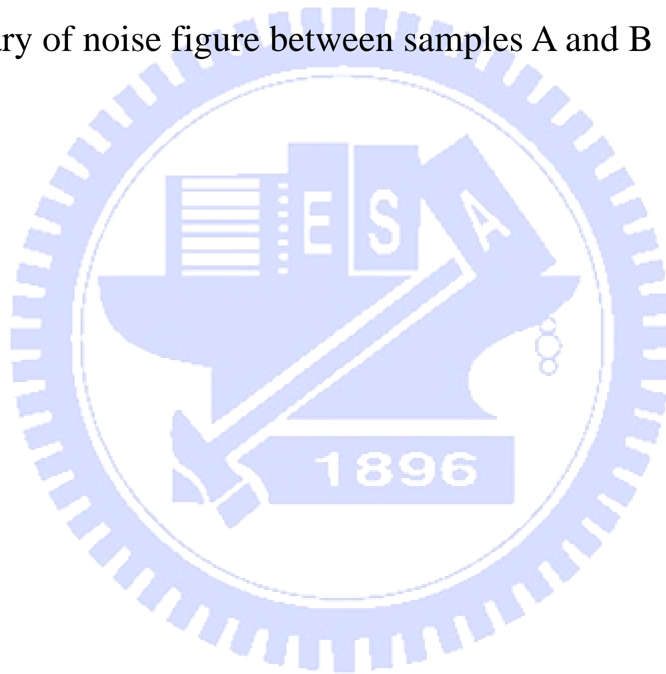

Figures

Fig.1.1 Conventional HEMT structure 8

Fig.1.2 Energy band gap v. s. lattice constant for the $In_xAl_{1-x}As/In_yGa_{1-y}As$ system 8

Fig.2.1 Energy band gap v.s. lattice constant for the $In_xAl_{1-x}Ga/In_yGa_{1-y}As$ system 12

Fig.2.2 Critical thickness curves corresponding to onset of 3D growth (h_{3D}), plastic relaxation through misfit dislocation (h_{MD}), and through 3D island dislocation (h_{ID}) as a function of In composition and growth temperature 12

Fig. 3.1 $(In_{0.53}Ga_{0.47}As)_m(InAs)_n$ super-lattice MHEMT structure 34

Fig. 3.2 Schematic of mesa etching 34

Fig. 3.3 Schematic of ohmic photo 35

Fig. 3.4 Schematic of the cross section of the device after ohmic metal (AuGe/Ni/Au) deposition 35

Fig. 3.5 Device layout of the sepsration MHEMT 36

Fig. 3.6 Drain current vs. RTA temperature 36

Fig. 3.7 Ohmic contact resistance of the superlattice MHEMT.................37

Fig. 3.8 Ebeam T-shaped gate followed by recess 38

Fig 3.9 SEM Micrograph of the cross section of the T-shaped gate profile....38

Fig. 3.10 Schematic of the device of the gate metal (Ti/Pt/Au) deposition.....39

Fig. 3.11 Schematic of the cross section of the device after SiN_x passivation 39

Fig. 3.12 SEM Micrograph of the device after SiNx passivation ....…40

Fig. 3.13 Schematic of the device after nitride via holes etching 40

Fig. 3.14 Schematic of the device after first photolithography for plating via holes...41

Fig. 3.15 Schematic of the device after thin metals Ti/Au deposition 41

Fig. 3.16 Schematic of the second photolithography for airbridge plating......41

Fig. 3.17 Schematic of the device after Au electroplating 42

Fig. 3.18 Schematic of the device after plating at Second photo-resist removal...42

Fig. 3.19 Schematic of the device after thin metal etching 42

Fig. 3.20 Schematic of the airbridge process after first photo-resist removal ..43

Fig. 3.21 (a) SEM photo of the side view of the airbridges (b) SEM photo of the front view of the airbridges.......................................43

Fig. 3.22 Band diagrams at three different locations along the channel of HEMT 44

Fig. 3.23 Actual I-V characteristics and those predicted by Eq. (3-4) 45

Fig. 3.24 (a) The side view of the TLM patterns, (b) The top view of TLM patterns. 45

Fig. 3.25 The illustration of utilizing TLM to measure ohmic contact resistance 46

Fig. 3.26 The equivalent two-port network schematic at low frequency 46

Fig. 3.27 The equivalent two-port network schematic at high frequency 47

Fig 3.28 Small signal representation of a common source FET 47

Fig.3.29 Definition of Cutoff Frequency f_T 48

Fig. 4.1 Drain-source current vs. drain-source voltage of (a) sample A and (b) sample B 55

Fig. 4.2 Transconductance vs. gate-source voltage of (a) sample A and (b) sample B 56

Fig. 4.3 Breakdown voltage, V_{br} of (a) sample A and (b) sample B 57

Fig. 4.4 Band diagrams for: (a) depletion, (b) flat-band, and (c) accumulation Indicate the effect of the barrier between the gate and channel on

hole extraction by the gate electrode……………………………….58

Fig.4.5 Gate-source voltage, V_{gs} vs. gate current, I_g of sample A ………….58

Fig. 4.6 Maximum available/stable power gain and current gain of
(a) sample A and (b) sample B ……………………………………..59

Fig. 4.7 F_{min} vs. I_{ds} at 16GHz of (a) sample A and (b) sample B …………...60

Fig. 4.8 Noise figure vs. frequency of samples A and B …………………...61